Optimization and characterization of synthesis of silver nanoparticles from *Manihot esculenta* Crantz L. petiole and leaf aqueous extracts and its antibacterial activity

Bung-on Prajanban[1], Sirilak Kamonwannasit[2], Santi Phosi[3], Agarat Kamcharoen[2*]

[1]Division of Agricultural Innovation, Faculty of Agricultural Technology, Burapha University Sakaeo Campus, Sa Kaeo 27160

[2]Division of Agro-Industrial Product Development, Faculty of Agricultural Technology, Burapha University Sakaeo Campus, Sa Kaeo 27610

[3]Department of Chemical Engineering, Faculty of Engineering, Burapha University, Chonburi 20131

[*]**Corresponding author:** agratk@buu.ac.th

Received: 18 December 2024/ Revised: 12 April 2025/ Accepted: 18 April 2025

Abstract

The objective of this study was to investigate the structure and antibacterial activity of silver nanoparticles (AgNPs) synthesized from the petioles and leaves of *Manihot esculenta* Crantz L. using hot water extraction (PMH and LMH extract, respectively). Optimal synthesis of AgNPs was criticized from UV-vis absorption spectra. For AgNPs synthesized from PMH extract (AgPMH), the synthesis was carried out by addition of 2 mg/mL of the PMH extract pH 12.0 with 4 mM silver nitrate solution in a 2:8 (v/v) ratio at a temperature of 60 °C for 120 min. For AgNPs synthesized from LMH extract (AgLMH), the synthesis was carried by the addition 2 mg/mL of LMH extract pH 10.0 with 4 mM silver nitrate solution in 2:8 (v/v) ratio at temperature 80 °C for 120 min. The change of Fourier-transform infrared (FTIR) spectra indicated that the AgNPs of both extracts were synthesized. Transmission electron microscopy (TEM) analysis revealed that the synthesized nanoparticles were within 15.27 to 95.58 nm in size for AgPMH and 3.98 to 23.23 nm for AgLMH. X-ray diffraction (XRD) results showed that nanoparticle formed were crystalline with face centered cubic geometry. Both synthesized AgNPs did not show activity against *Escherichia coli* and *Bacillus cereus.*

Keywords: *Manihot esculenta* Crantz L., Silver nanoparticles, Green synthesis, Hot water extraction

Introduction

There are a lot of methods for the synthesis of silver nanoparticles such as chemical and green synthesis. Compared to chemical methods, the green synthesis is an inexpensive, eco-friendly, easier alternative approach and less hazardous. The chemical method requires external stabilizer agent to protect nanoparticles from aggregation and reducing agents to reduce Ag^{+} to Ag^{0} to synthesize silver nanoparticles such as sodium borohydrate and sodium citrate. Plant extracts can act as both reducing and stabilizing

agents for metal nanoparticles [1]. Generally, organic substances in plant such as primary and secondary metabolites are able to reduce metal ions into nanoparticles and stabilize those of synthesized particles [2]. However, the properties of metallic nanoparticles synthesized through green methods are significantly influenced by the specific part of the plant utilized, because of the diverse phytochemical compositions' present [3]. Numerous variables including the concentration, pH, duration of incubation, and temperature of the plant extract effected to the formation of metal ions into nanoparticles and to regulate their size have documented [4].

Silver nanoparticles (AgNPs) have demonstrated highly antibacterial action against multiple Gram-positive and Gram-negative bacteria [5]. The stability of the product formed is a significant factor in the final antibacterial activity, along with the size and charge of the nanoparticles [6]. The bactericidal and bacteriostatic capacity of nanoparticles between 5 and 100 nm was evaluated against Gram-negative and Gram-positive bacteria [7]. The electrostatic attraction between AgNPs and negatively charged bacterial cells is crucial to their antibacterial effectiveness, and it is controlled by both AgNPs' and microorganisms' charges [8]. If AgNPs are unstable, they will tend to aggregate and form larger particles leading to lower antibacterial activity [6]. Interestingly, the highest uptake and translocation of silver (Ag) was observed in leaf extract [9], which has shown an antimicrobial activity. Ajitha et al. [10] prepared AgNPs using *Plectranthus amboinicus* leaf extract. The morphology of the nanoparticles showed the formation of nearly spherical nanoparticles which showed effective antibacterial capacity against *Escherichia coli* and *Penicillium* spp. The biosynthesis of AgNPs was conducted using the leaf extract of plant *Protium serratum*. The potential antibacterial activity of AgNPs (size 74.56±0.46 nm) was studied against the food borne pathogens such as *Pseudomonas aeruginosa*, *E. coli* and *Bacillus subtilis* [11]. The leaf aqueous extract of *Jatropha curcas* was used for the synthesis of AgNPs. The TEM analysis clearly showed variation in particle shape and size (20–50nm). While majority of the nanoparticles were spherical, some showed irregular shapes and edges. Which showed against *E. coli*, *Staphylococcus aureus*, and *Salmonella enterica* [12].

Manihot esculenta Crantz L. also called cassava is an economic crop of in Thailand. The leaf is not well known to serve as a major source of vegetable. Thus, it is often discarded as waste after harvesting the tubers [13]. Cassava leaves contain phytochemicals such as alkaloids [14], flavonoids [14-16], phenolic compounds [14, 16], tannins [14] and saponins [14] that may have the capability of capping and reducing the nanoparticles [17] for towards a potential commercial scale. Cassava leaves have the ability to against *S. epidermidis* and *Propionibacterium acnes* [15]. Velayutham et al. [18] reported that AgNPs synthesis using leaf aqueous extract of cassava against two important mosquito species, *Aedes aegypti* and *Culex quinquefasciatus*. However, there has never been a report on the synthesis of AgNPs from cassava leaves for inhibiting bacteria. The objective of this work was to investigate the structure-activity relationship of green-synthesized AgNPs, derived from the petiole (PMH) and leaves (LMH) of *Manihot esculenta* Crantz L. through hot water extraction, with respect to their antibacterial properties.

Materials and Methods

1. Preparation of *Manihot esculenta* Crantz L.

Manihot esculenta Crantz L. Leaves were collected from agricultural lands at Huai Jot Subdistrict in Wattana Nakorn District, Sa Kaeo Province. A young and mature leaf was selected in each tree from cassava aged between 10 and 12 months in October to December 2023.

Petiole and leaf were separated and washed several times in water to remove dirt. These were cut into small pieces and then dried using a hot air oven at 50°C for 2 days. The dried pieces were mashed. Petiole and leaf were extracted by distilled water at 80°C for 1 h. The extraction liquid parts were filtrated, concentrated, and kept at 4°C. The extract from hot water extraction was called petiole *of M. esculenta* hot water extract (PMH) and leaf *of M. esculenta* hot water extract (LMH).

2. Synthesis of silver nanoparticles

Optimization of silver nanoparticles (AgNPs) production under different reaction conditions includes variations in pH (pH 5-12), silver nitrate concentrations (0.5, 1.0, 2.0 and 4.0 mM), extract concentrations (0.25, 0.5, 1.0 and 2 mg/ml), ratios of extract and silver nitrate (1:9, 2:8, 3:7, 4:6, 5:5, 6:4, 7:3, 8:2 and 9:1 v/v), temperature (40, 50, 60, 70 and 80°C) and time interval (0, 30, 60, 90, 120, 150, 180, 210, 240, 360 and 480 min), respectively. While optimizing each parameter, the other parameters remain stable. All reactions were conducted in a dark environment to prevent the photoactivation of the mixture. Each experiment was carried out at least in triplicate. The AgNPs synthesis was monitored by recording UV-vis spectra (λ 300 - 600 nm) using a NanoDrop 2000 C spectrophotometer (Thermo Fischer, USA).

The AgNPs was isolated from the optimized mixture as follows. The obtained reaction mixture was centrifuged at 10,000 × g for 15 min. The pellet was purified using deionized water and washed repeatedly to ensure better separation of free entities from the AgNPs. The obtained AgNPs were lyophilized and used for further characterization and its antibacterial activity.

3. Characterization of AgNPs

Fourier transform infrared spectroscopy (Bruker Tensor 27 FT-IR spectrometer) spectra of the AgNPs were recorded in the diffuse reflectance mode at a resolution of 4 particles cm^{-1}, then were analyzed with Optical User Software (OPUS) 7.5 (Bruker Optics Ltd, Ettlingen, Germany). XRD analysis of AgNPs was carried out by EMPYREAN model, PANalytical instrument (45 kV, 40 mA) using CuKα radiation with λ of 1.5406 Å and a nickel monochromator filtering wave operating at a tube voltage of 45 kV and a tube current of 40 mA. The scanning was performed in the 2θ range of 5°– 90° at step size 0.02 degree with a time constant of 30 s/step. Moreover, the morphologies, crystalline natures, and size distributions of the AgNPs were determined using Transmission electron microscopy (TEM) and Image J program. The results were expressed as mean ± standard deviation.

4. The disc diffusion method

The antimicrobial susceptibility of AgNPs was evaluated using the disc diffusion. This method was performed in Mueller Hinton Agar (MHA). Silver nanoparticles of 800 µg/mL and the extract (PMH or LMH) of 10 mg/mL were filtered with a 0.2 µM syringe filter. Ten microliters of AgNPs and extracts were dropped

onto the sterile dish, and was placed on *E. coli* and *B. cereus* cultured agar plate, were then incubated for 24 h at 37°C and inhibition zone was monitored.

Results and Discussion

The change in the color of reaction mixture to dark brown after mixing a plant extract and silver nitrate is a general characteristic of silver nanoparticle biosynthesis [19]. The formation of AgNPs was observed using UV–visible spectroscopy. Figure 1a–f and Figure 2a-f shows the absorption spectra in the AgNPs synthesized under different reaction parameters such as pH, silver nitrate concentrations ($AgNO_3$), extract concentrations, ratios of extract and silver nitrate, temperature, and time of PMH extract and LMH extract, respectively. The first factor considered was pH; variations of pH 5-12 mixed with the extract at concentration of 1 mg/mL and silver nitrate concentration of 2 mM in a 1:1 ratio was incubated at room temperature for 1 h. The pH of the solution primarily affects the surface charge of phytochemical functional groups [20] of PMH and LMH extract. At acidic pH did not show the characteristic peak for the AgNPs synthesis using both PMH and LMH extracts. The alkaline pH 11-12 has exhibited peak for the AgNPs synthesis from PMH extract (AgPMH). The maximum absorption was determined at pH 12 as shown in Figure 1a, AgNPs in colloidal solutions display maximum absorption in the λ 350–500 nm range. The alkaline pH 8-12 has exhibited peak for the AgNPs synthesis from LMH extract (AgLMH). The maximum absorption was determined at pH 10 as shown in Figure 2a, AgNPs display maximum absorption in the λ 350–475 nm range. AgNPs synthesis occurs only at strongly alkaline conditions may be due to deposition of hydroxides on AgNPs [21]. The second factor considered was concentration of silver nitrate, the PMH concentration of 1 mg/mL at pH 12 or the LMH concentration of 1 mg/mL at pH 10 mixed with various $AgNO_3$ concentrations in a 1:1 ratio incubated at room temperature for 1 h. The peak absorbance persistently increased with increase in concentrations from 0.5 to 4.0 mM, representing the parallel relationship with the metal ion concentration of the AgPMH and AgLMH (Figure 1b and Figure 2b). Liaqat et al. [22] reported that the optimum concentration of $AgNO_3$ was 1mM because the shifting of the surface plasmon resonance (SPR) peaks of AgNPs at a high concentration of $AgNO_3$ (2 mM) indicated this was unsuitable for the synthesis of AgNPs. The UV spectrum exhibits the highest peak at an $AgNO_3$ concentration of 6 mM, indicating optimal synthesis conditions. Moreover, an increase in Ag^+ does not alter the position of the SPR peak within a concentration range of 4–8 mM $AgNO_3$ [23]. In addition, the position and width of the peaks also change, indicating that the higher $AgNO_3$ concentration does affect the size and morphology of AgNPs. For this reason, $AgNO_3$ concentration of 4 mM was selected to further study.

The third factor to evaluate the effect of plant extract concentrations (0.25-2 mg/mL) was mixed with 4 mM $AgNO_3$ at a pH of 12 for PMH or at a pH of 10 for LMH in a 1:1 ratio and room temperature for 1 h. The increase in the concentration of the leaf extract will also increase the absorbance intensity. This result may be due to an increase the number of bio-compounds requiring to reduce Ag^+ to Ag^0 [23]. The intensities of absorbance maximums increased with an increase in the concentrations of extract from 0.25 to 2.0 mg/mL of PMH (Figure 1c), and from 1.0 to 2.0 mg/mL of LMH (Figure 2c). We got a maximum yield and decreased width of the peaks with 2.0 mg/mL of both PMH and LMH extract concentrations.

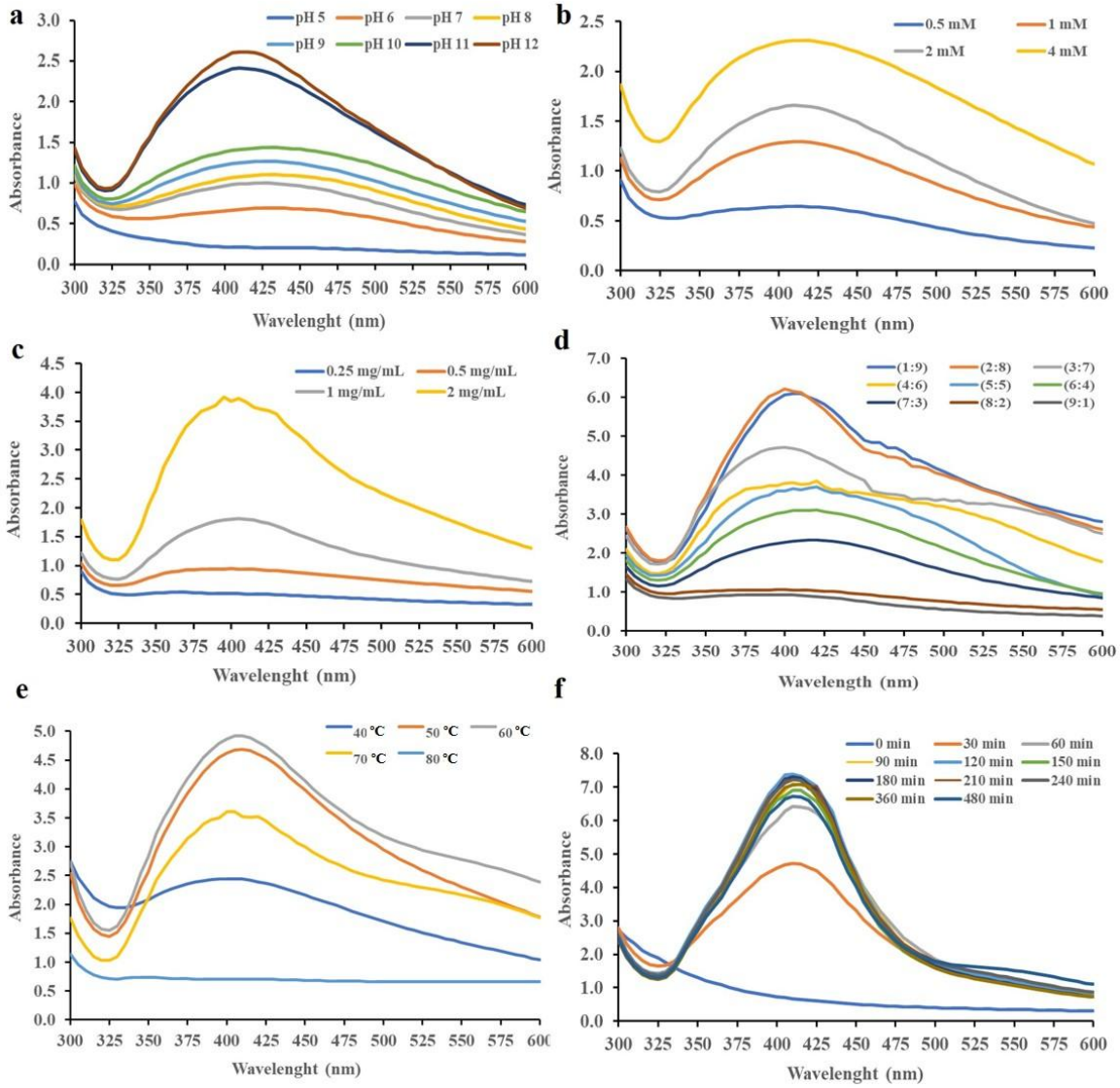

Figure 1 UV-vis absorption spectra of optimizing parameters to produce AgNPs with different pHs (a), concentrations of silver nitrate ($AgNO_3$) (b), concentrations of PMH (c), ratios of extract and silver nitrate (d), temperature (e) and time (f).

The fourth factor was the ratio of the extract concentrations of 2.0 mg/mL (pH 12 of PMH, pH 10 of LMH) and 4 mM $AgNO_3$ with different ratios and incubated at room temperature for 1 h. Which was altered to investigate the optimum composition to maximize of the AgNPs. In general, intensities of absorbance increased with in extract from 10 to 50%, whereas absorbance decreased with a decrease in extract from 60 to 10% [24]. For the PMH extract, the highest absorbance with a comparatively narrow peak was observed when both reactants were used in 2:8 (v/v) ratio (Figure 1 d). However, for the LMH extract, the highest absorbance with a comparatively broad peak was observed when both reactants were used in 2:8 (v/v) ratio (Figure 2 d). Ali et al. [24] reported that the highest absorbance with a comparatively narrow peak was observed when both reactants were used in 1:1 (v/v) ratio of plant extract and $AgNO_3$. The shapes of the absorption peaks remain changed for AgNPs using PMH and LMH synthesis, indicating that the reaction ratio of plant extract with $AgNO_3$ does affect the size and morphology of AgNPs.

The fifth factor was various temperature. Both of 2 mg/mL of PMH at pH 12 and 2 mg/mL of LMH at pH 10 were mixed with 2 mM $AgNO_3$ in a 2:8 ratio at different temperatures for 1 h. The peaks were found in the range of 350–475 nm for AgNPs synthesized at 40-70°C using PMH extract. The highest absorbance peak was observed when temperature was used in 60°C (Figure 1e). The rise in temperature not only decreased the absorbance but also shifted the λ_{max} [23]. Under identical conditions, a temperature of 40-60°C yields decreased a more intense peak than synthesis at room temperature, suggesting the generation of a smaller amount of AgNPs. However, a temperature of 40-60°C shown smoot peak more than synthesis at room temperature. Ni et al. [20] reported a temperature of 90°C yields a more intense SPR peak than synthesis at room temperature, suggesting the generation of a larger amount of AgNPs. By the way, peaks were found in the range of 350–475 nm for silver nanoparticles synthesized at 40-80°C using LMH extract. The highest absorbance peak was observed when temperature was used in 80°C (Figure 2e).

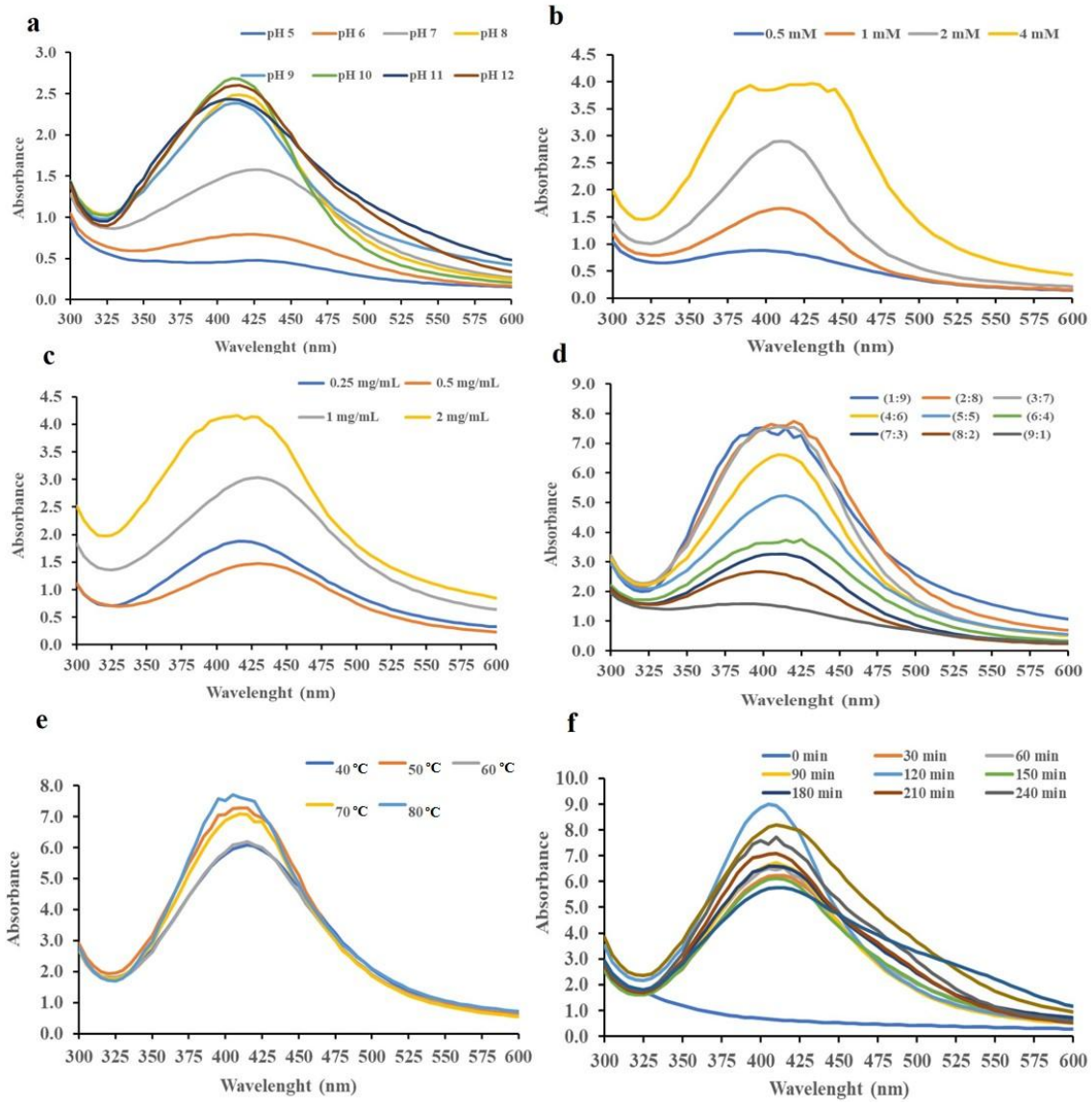

Figure 2 UV-vis absorption spectra of optimizing parameters to produce AgNPs with different pHs (a), concentration of silver nitrate ($AgNO_3$) (b), concentration of LMH (c), ratios of extract and silver nitrate (d), temperature (e) and time (f).

Increase in temperature from 25°C to 75°C resulted in an increase in the absorbance, indicating an increased synthesis rate of AgNPs [23]. Under identical conditions, a temperature of 80°C yields a similar synthesis at room temperature but a narrower peak than synthesis at room temperature. The position and width of the peaks also change, indicating that the temperature does affect the size and morphology of AgNPs. The sixth factor was the time required for the completion of the reaction: 2 mg/mL of PMH pH 12 or LMH pH 10 mixed with 4 mM $AgNO_3$ in a 2:8 ratio incubated at 60°C for PMH and at 80°C for LMH with different times.

As the duration of reaction increases, more silver nanoparticles are formed within 30 min and it continued turning darker with time. Time–course analysis of UV–vis data of plant extract:$AgNO_3$ (1:1 v/v) mixture showed accumulation of AgNPs within an hour of the reaction start time [23]. The results shown in Figure 1f and Figure 2f demonstrate that the synthesis of AgNPs is completed within 120 min. With increasing reaction time, the nucleation of NPs occurs at a slower rate. The shapes of the absorption peaks remain unchanged for AgNPs using PMH synthesis, indicating that the reaction time does not affect the size and morphology of AgNPs that correlated with previously reported [20]. However, the shapes of the absorption peaks remain changed for AgNPs using LMH synthesis, indicating that the reaction time does affect the size and morphology of AgNPs.

FTIR spectra of $AgNO_3$, PMH extract, LMH extract and synthesized AgNPs are shown in Figure 3. In $AgNO_3$, the peaks are observed at 808, 1034, 1280 and 1624 cm^{-1}. In PMH extract, the peaks are observed at 920, 989, 1047, 1407 and 1594 cm^{-1}. After reaction with $AgNO_3$, the peaks are shifted, such as 992, 1350 and 1559 cm^{-1}. In LMH extract, the peaks are observed at 1032, 1392 and 1599 cm^{-1}. After reaction with $AgNO_3$, the peaks are shifted, such as 1047, 1375 and 1579 cm^{-1}, respectively. The FTIR spectra of PMH and LMH extract shows the peaks at 1047 and 1032 cm^{-1}, respectively. These correspond to the position of sapogenin linked with oligosaccharides, consistent with the presence of saponin compounds as components in the extract. The FTIR spectra of saponin shows the peaks at 1076 cm^{-1} (C-O-C stretching of glycoside linkage of oligosaccharide to sapogenin) [25]. Oligosaccharide linkage absorptions to sapogenins (C-O-C) were at 1074 cm^{-1} and between 1045 cm^{-1} to 1046 cm^{-1}. This result was similar with previous works, the C-O-C absorbance was observed at ~1034.78 cm^{-1} and 1033.22 cm^{-1} in the water extracts of *Sapindus rarak* and *Litsea glutinosa,* respectively [26]. In addition, In PMH extract, the peaks are observed at 920, 989, 1047, 1407 and 1594 cm^{-1} while the LMH extract the peaks are observed at 1032, 1392, and 1599 cm^{-1}. These results may be due to the vibration of polysaccharide compounds in the PMH and LMH extracts, which are the absorption regions of polysaccharides: region II in the range of 1800–1500 cm^{-1}, region III in the range of 1500–1200 cm^{-1}, and region IV in the range of 1200–800 cm^{-1} [27]. Therefore, when synthesized into AgNPs, the peaks are similar to the extract samples and resemble the $AgNO_3$.

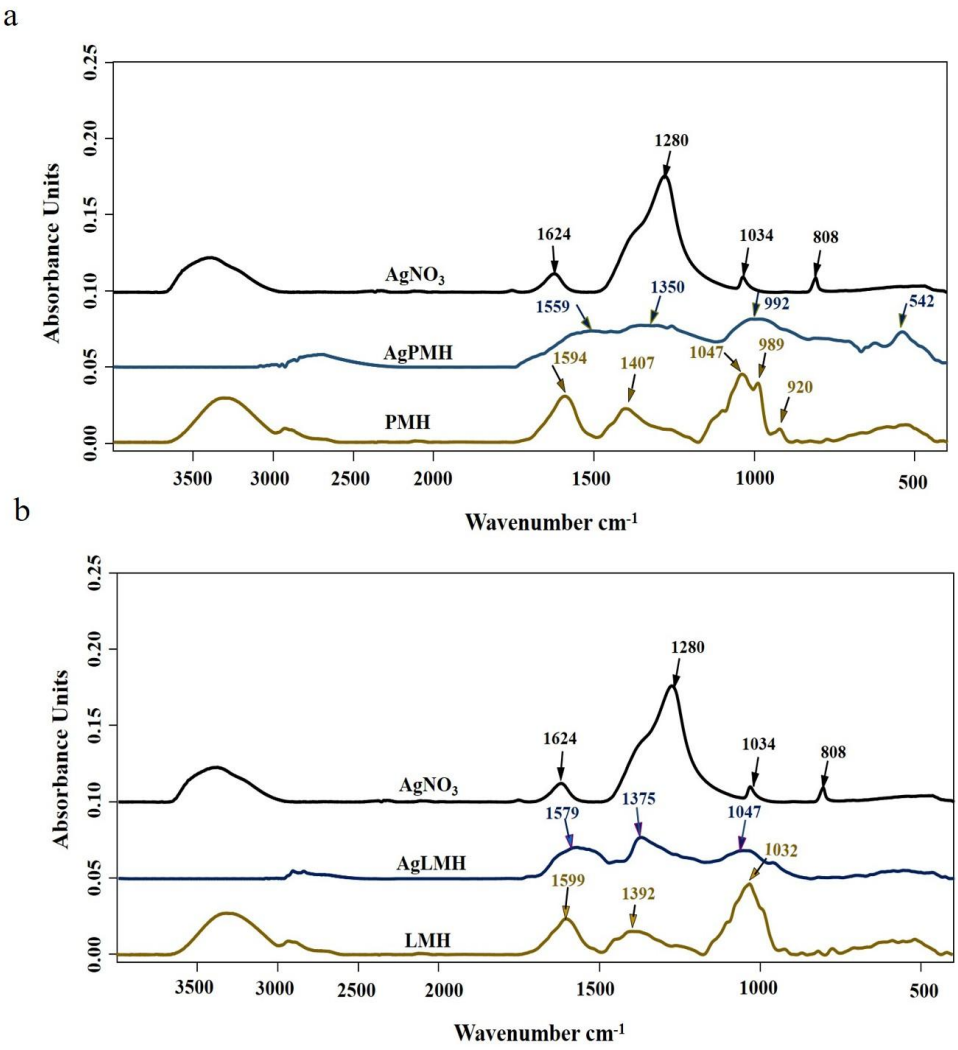

Figure 3 FTIR spectra of $AgNO_3$, PMH extract and AgPMH synthesized at optimum parameters (a), LMH extract and AgLMH synthesized at optimum parameters (b).

The sizes and shapes of AgNPs were analyzed using TEM. The shape of AgPMH was spherical and oval-like spherical with an average size of 15.27–95.58 nm (40.46 ± 13.49 nm) with aggregation (Figure 4). The shape of the AgLMH was in spherical and oval like spherical with an average size of 3.98–23.23 nm (10.16±2.8 nm) with little aggregation (Figure 5). The diameters of AgNPs produced by *M. esculenta* ranged from 13 to 38 nm, with an average of 23.0 nm [28]. The higher content of OH- species in the basic condition may facilitate the deprotonation of -COOH groups to -COO-, allowing the adsorption of Ag^+ ions by electrostatic attraction or affinity interaction [29]. Basic pH generally formed AgNPs with smaller and narrower size distribution [29]. As a result, the formation of AgLMH will most likely occur in more small size and distribution than AgPMH. Nevertheless, the increasing particle size and narrower size distribution was proportionally affected by the increasing pH since the pattern observed was fluctuating in AgPMH. Small spherical particles are obtained at high pH values. However, in certain experimental scenarios described in the literature, higher pH levels have resulted in size growth, particle aggregation, and reduced synthesis rates of AgNPs [30] The size of the synthesized silver particles increases with the rising concentration of $AgNO_3$.

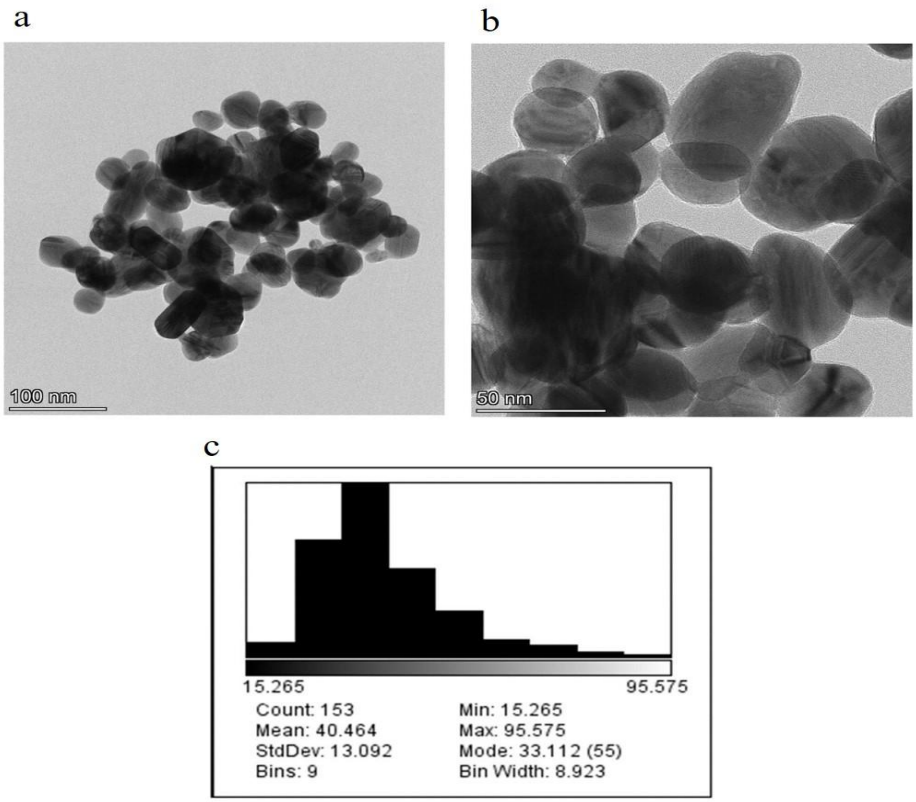

Figure 4 Transmission electron microscopy (TEM) images of AgNPs synthesized with PMH extract, at 100 nm (a), 50 nm (b) and particle distribution size (c).

The variation of $AgNO_3$ concentration (0.5, 1, 2, 4, 6, 8, and 10 mM) were investigated to synthesize AgNPs with using aqueous leaf extract of *Ziziphus spina–Christi,* indicates an increase in the size of particles (25-42 nm) as confirmed by TEM [31]. In addition, the plant extract concentration used also plays important role in the conversion of Ag^+ to Ag^0. This deviation in particle size clearly suggests that at higher plant extract concentration, there is more presence of reducing agents present in the extract compared to reactant which tends to increase the particle size upon longer exposure duration [32]. In our study, it was used in a 2:8 (v/v) ratio of the extract concentration 2.0 mg/mL and silver nitrate concentration 4 mM. This suggests that small amounts of the extract can reduce silver ions, but do not protect most of the quasi-spherical nanoparticles from aggregation because of the deficiency of biomolecules to act as protecting agents. However, the biomolecules function as reducing agents and cap the nanoparticle surfaces at higher extract concentrations, preventing them from aggregation [33]. Moreover, a change in particle size was observed when higher concentrated $AgNO_3$ was used [34-35]. An average particle size of 33 nm at 50°C, 29 nm at 70°C, and 26 nm at 90°C, particle sizes was decreased with increasing temperature [36]. The TEM results indicate that the samples obtained over a longer period retained a narrower particle size distribution; the average size of all prepared Ag-NPs was less than 20 nm [37].

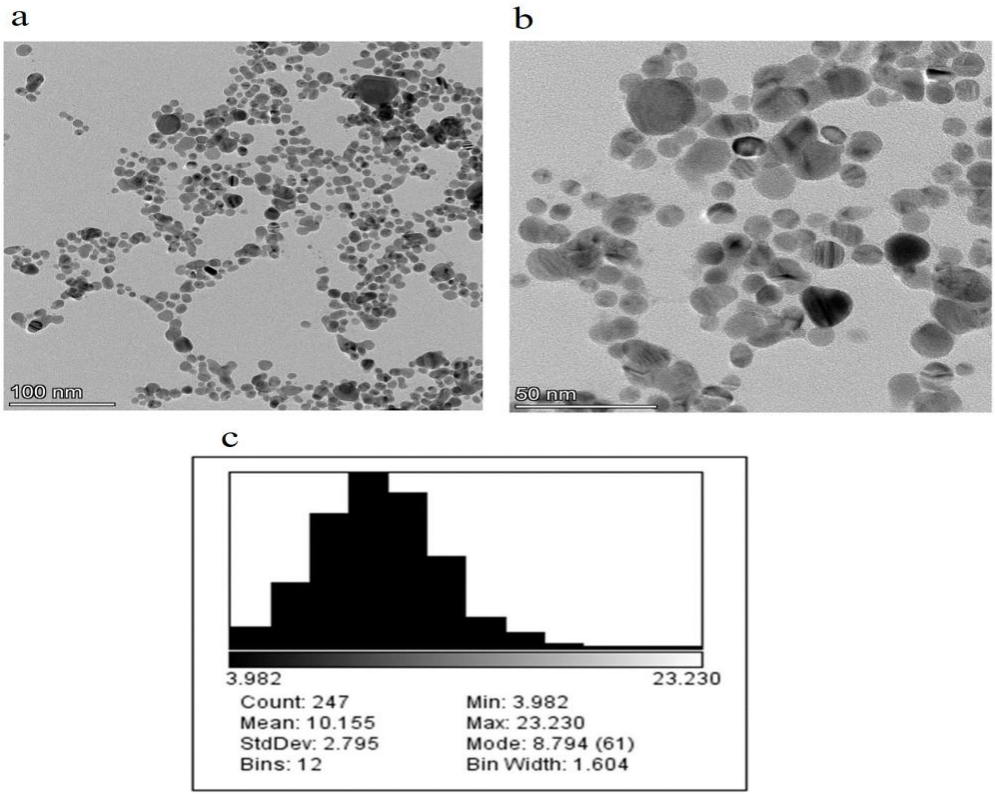

Figure 5 Transmission electron microscopy (TEM) images of AgNPs synthesized with LMH extract, at 100 nm (a), 50 nm (b) and particle distribution size (c).

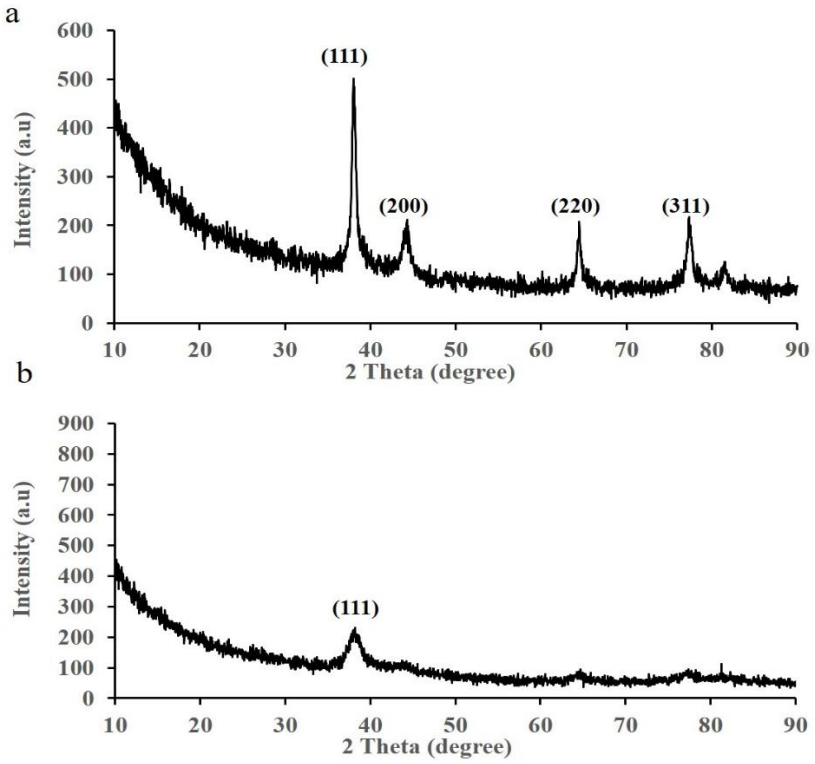

Figure 6 XRD patterns of the AgNPs synthesized at optimum parameters of PMH extract (a) and LMH extract (b).

Figure 6 shows the XRD pattern of silver nanoparticles. Figure 6a is apparent that characteristic diffraction peaks at (111), (200), (220) and (311) in 2θ corresponds to lattices of (38.03°), (44.28°), (65.33°) and (77.31°), respectively. These peaks and planes of reflections are matched with the ICDD (International Centre for Difraction Data) PDF (Powder Difraction File) 04-0783 for Ag [35]. A similar result was observed by Anandalakshmi et al. [23], who identified crystalline peaks 38.11, 44.22, 64.45 and 77.40 corresponding to the (111), (200), (220) and (311) planes, respectively. The typical pattern of green-synthesized AgNPs is found to possess a face-centered cubic (FCC) structure [23]. Figure 6b is apparent that characteristic diffraction peaks at (111) in 2θ corresponds to lattices of (38.21°). Raja et al. [38] reported that the XRD patterns of tannin-silver nanoparticles show a sharp peak at 38°, which corresponds to the peak at (111) of the cubic silver structures within experimental error. Due to the product's low silver nanoparticle concentration, only one or two peaks are visible [38].

AgNPs, PMH and LMH extracts have been shown to be not effective against *E. coli* and *B. cereus* (Figure 7). On the other hand, fresh and dried (*M. esculenta*) leaf extract was added with varying concentrations of 5%, 10%, 20% and 30% ethanol. These extracts have shown to be effective against *E. coli* [39]. AgNPs synthesized using *M. esculenta*, can act as an antibacterial agent against *E. coli* and *B. cereus* [28]. The antibacterial activity was significantly reliant on size, relation attributed to the larger surface area of the smaller nanoparticles, available to direct contact with the bacterial cell [7]. If the synthesized AgNPs have low stability, they will tend to aggregate and form bigger particles, and as has been shown, nanoparticles with bigger sizes have lower antibacterial activity [6]. AgNPs were synthesized from the leaf extract of Ginkgo biloba, exhibited a spherical morphology, uniform dispersion, and diameter ranging from ~8 to 9 nm which against both Gram-positive and Gram-negative strains at low AgNP concentrations [20].

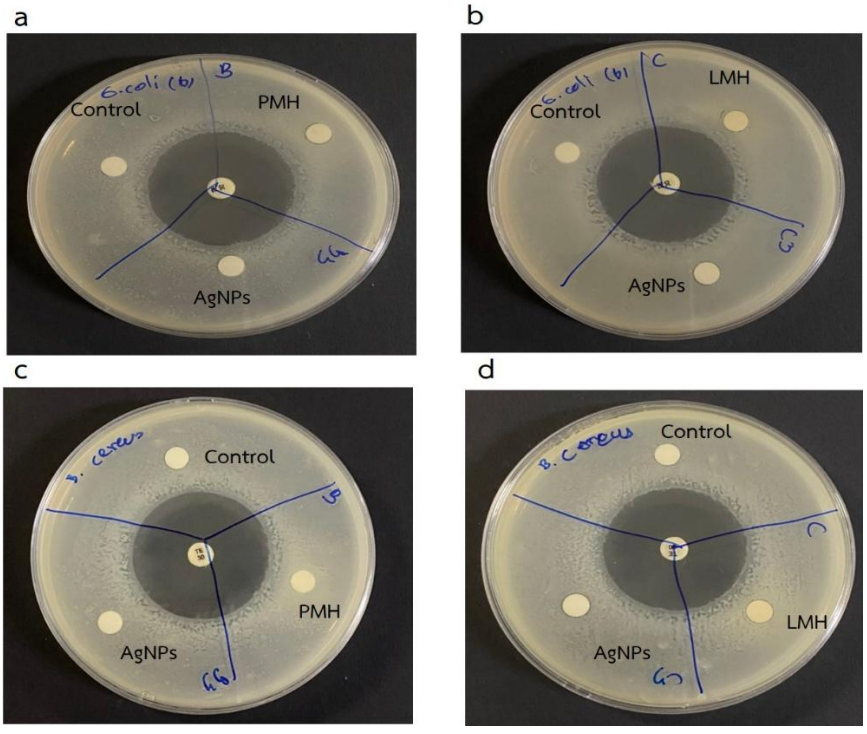

Figure 7 Zones of inhibition of AgNPs, PMH and LMH extracts against *E. coli* (a and b) and *B. cereus* (c and d).

Thus, AgNPs was synthesized from using PMH and LMH not effective against *E. coli* and *B. cereus* should be a cause of used high pH, high concentration of $AgNO_3$, high concentration of PMH, ratio of extract with $AgNO_3$ temperature and time leading to increased particle sizes and not uniform dispersion unavailable to contact with the bacterial cell.

Conclusion

In our study, the method for biological synthesis of silver nanoparticles by *M. esculenta* petiole and leaf aqueous extracts was established. AgNPs synthesized from PMH extract (AgPMH) was carried out by the addition of 2 mg/mL of the petiole extract pH 12.0 with 4 mM silver nitrate solution in a 2:8 (v/v) ratio at a temperature of 60 °C for 120 min. For AgNPs synthesized from LMH (AgLMH) extract, synthesis was carried by the addition 2 mg/mL of leaf extract pH 10.0 with 4 mM silver nitrate solution in 2:8 (v/v) ratio at temperature 80 °C for 120 min. The change of FTIR spectra indicated that the silver nanoparticles of both PMH and LMH were synthesized. TEM analysis revealed that the synthesized nanoparticles were within 15.27 to 95.58 nm in size for AgPMH with aggregation, and 3.98 to 23.23 nm for AgLMH with little aggregation. XRD results showed that nanoparticles formed crystalline with face centered cubic geometry. This result demonstrated that the silver nanoparticles obtained by extracts not effective against *E. coli* and *B. cereus*. This biogenic process of synthesis AgNPs by using PMH and LMH extracts will be helpful for adjusting methodologies for increase stability advantageous in against microorganisms. Moreover, another biological function should be further studied. That will develop AgNPs for biomedical applications and the food industry.

Acknowledgements

This work was financially supported by (i) Burapha University (BUU), (ii) Thailand Science Research and Innovation (TSRI), and (iii) National Science Research and Innovation Fund (NSRF) (Fundamental Fund: Grant no.53/2566). Thank you for Faculty of Agricultural Technology, Burapha University Sakaeo Campus and Faculty of Engineering, Burapha University, Chonburi, for instrumental facility.

References

1. Jalab J, Abdelwahed W, Kitaz A, Al-Kayali, R. Green synthesis of silver nanoparticles using aqueous extract of *Acacia cyanophylla* and its antibacterial activity. Heliyon, 2021;7(9):e08033.
2. Miranda A, Akpobolokemi T, Chung E, Ren G, Raimi-Abraham BT. pH alteration in plant mediated green synthesis and its resultant impact on antimicrobial properties of silver nanoparticles (AgNPs). Antibiotics (Basel) 2022;11(11):1592.
3. Silva LP, Reis IG, Bonatto CC. Green synthesis of metal nanoparticles by plants: current trends and challenges. In green processes for nanotechnology; Springer: New York, NY, USA; 2015:259–75.
4. Patra JK, Baek KH. Green nanobiotechnology: factors affecting synthesis and characterization techniques. J Nanomater 2014;2014(1):417305.

5. Cavassin ED, de Figueiredo LFP, Otoch JP, Seckler MM, de Oliveira RA, Franco FF, Marangoni VS, Zucolotto V, Levin ASS, Costa SF. Comparison of methods to detect the in vitro activity of silver nanoparticles (AgNP) against multidrug resistant bacteria. J Nanobiotechnol 2015;13:1–16.
6. Chen J, Li S, Luo J, Wang R, Ding W. Enhancement of the antibacterial activity of silver nanoparticles against phytopathogenic bacterium *Ralstonia solanacearum* by stabilization. J Nanomate 2016;2016(1):7135852.
7. Agnihotri S, Mukherji S, Mukherji S. Size-controlled silver nanoparticles synthesized over the range 5–100 nm using the same protocol and their antibacterial efficacy. RSC Adv 2014;4:3974–83.
8. Abbaszadegan A, Ghahramani Y, Gholami A, Hemmateenejad B, Dorostkar S, Nabavizadeh M, Sharghi H. The effect of charge at the surface of silver nanoparticles on antimicrobial activity against gram-positive and gram-negative bacteria: A Preliminary Study. J Nanomater 2015;2015:720654.
9. Marchiol L, Mattiello A, Poš´ci´c F, Giordano C, Musetti R. In Vivo synthesis of nanomaterials in plants-location of silver nanoparticles and plant metabolism. Nanoscale Res Lett 2014;9:101.
10. Ajitha B, Ashok Kumar Reddy Y, Sreedhara Reddy P. Biosynthesis of silver nanoparticles using *Plectranthus amboinicus* leaf extract and its antimicrobial activity. Spectrochim Acta A Mol Biomol Spectrosc 2014;128:257-62.
11. Mohanta YK, Panda SK, Bastia AK, Mohanta TK. Biosynthesis of silver nanoparticles from *Protium serratum* and investigation of their potential impacts on food safety and control. Front Microbiol 2017;8:626.
12. Chauhan N, Tyagi AK, Kumar P, Malik A. Antibacterial potential of *Jatropha curcas* synthesized silver nanoparticles against food borne pathogens. Front Microbiol 2016;7:1748.
13. Essien ER, Atasie VN, Okeafor AO, Nwude DO. Biogenic synthesis of magnesium oxide nanoparticles using *Manihot esculenta* (Crantz) leaf extract. Int Nano Lett 2020;10(1):43-48.
14. Appiah H, Falah S. Dewi, LK. Effect of boiled cassava leaves (*Manihot esculenta* Crantz) on total phenolic, flavonoid and its antioxidant activity. Curr Biochem 2016;3(3):116-27.
15. Mustarichie R, Sulistyaningsih S, Runadi D. Antibacterial activity test of extracts and fractions of cassava leaves (*Manihot esculenta* Crantz) against clinical of *isolates Staphylococcus epidermidis* and *Propionibacterium acnes* causing acne. Int J Microbiol 2020;1975904.
16. Quartey E, Amoatey H, Achoribo E, Owusu-Ansah M, Nunekpeku W, Donkor S, Ofori ESKE. Phytochemical constituents and antioxidant activities in leaves of 14 breeding lines of cassava (*Manihot esculenta* Crantz). Am J Exp Agric 2016;12(5):1-10.
17. Tesfaye M, Gonfa Y, Tadesse G, Temesgen T, Periyasamy S. Green synthesis of silver nanoparticles using *Vernonia amygdalina* plant extract and its antimicrobial activities. Heliyon, 2023;9(6):e17356.
18. Velayutham K, Ramanibai R, Umadevi M. Green synthesis of silver nanoparticles using *Manihot esculenta* leaves against *Aedes aegypti* and *Culex quinquefasciatus*. J Basic Appl Zool 2016;74:37-40.
19. Velu M, Lee JH, Chang WS, Lovanh N, Park YJ, Jayanthi P, Palanivel V, Oh BT. Fabrication, optimization, and characterization of noble silver nanoparticles from sugarcane leaf (*Saccharum officinarum*) extract for antifungal application. 3 Biotech 2017;7(2):147.

20. Ni Q, Zhu T, Wang W, Guo D, Li Y, Chen T, Zhang, X. Green synthesis of narrow-size silver nanoparticles using *Ginkgo biloba* leaves: condition optimization, characterization, and antibacterial and cytotoxic activities. Int J Mol Sci 2024;25(3):1913.
21. Maria BS, Devadiga A, Kodialbail VS, Saidutta MB. Synthesis of silver nanoparticles using medicinal *Zizyphus xylopyrus* bark extract. Appl Nanosci 2015;5:755–62.
22. Liaqat N, Jahan N, Khalil-Ur-Rahman, Anwar T, Qureshi H. Green synthesized silver nanoparticles: Optimization, characterization, antimicrobial activity, and cytotoxicity study by hemolysis assay. Front Chem 2022;10:952006.
23. Anandalakshmi K, Venugobal J, Ramasamy VJAN. Characterization of silver nanoparticles by green synthesis method using *Pedalium murex* leaf extract and their antibacterial activity. Appl Nanosci 2016;6:399-408.
24. Ali M, Kim B, Belfield KD, Norman D, Brennan M, Ali GS. Green synthesis and characterization of silver nanoparticles using *Artemisia absinthium* aqueous extract-A comprehensive study. Mater Sci Eng C Mater Biol Appl 2016;58:359-65.
25. Bajad PN, Pardeshi AB, Pagore VP. Extraction, isolation and quantification of saponin from *Dodonaea viscosa* JACQ. Pharma Innovation 2019;8(5):41-4.
26. Wisetkomolmat J, Suksathan R, Puangpradab R, Kunasakdakul K, Jantanasakulwong K, Rachtanapun P, Sommano SR. Natural surfactant saponin from tissue of *Litsea glutinosa* and its alternative sustainable production. Plants 2020;9(11):1521.
27. Hong T, Yin JY, Nie SP, Xie MY. Applications of infrared spectroscopy in polysaccharide structural analysis: Progress, challenge and perspective. Food Chem X 2021;12:100168.
28. Syafiuddin A, Salmiati, Hadibarata T, Salim MR, Kueh ABH, Sari AA. A purely green synthesis of silver nanoparticles using *Carica papaya, Manihot esculenta*, and *Morinda citrifolia*: synthesis and antibacterial evaluations. Bioprocess Biosyst Eng 2017;40(9):1349-1361.
29. Miranda A, Akpobolokemi T, Chung E, Ren G, Raimi-Abraham, BT. pH alteration in plant-mediated green synthesis and its resultant impact on antimicrobial properties of silver nanoparticles (AgNPs). Antibiotics (Basel) 2022;11(11):1592.
30. Nahar K, Rahaman MH, Khan GM, Islam M, Al-Reza, S. Green synthesis of silver nanoparticles from *Citrus sinensis* peel extract and its antibacterial potential. Asian J Green Chem. 2020;5:135–150.
31. Bamsaoud SF, Basuliman MM, Bin-Hameed EA, Balakhm SM, Alkalali AS. The effect of volume and concentration of $AgNO_3$ aqueous solutions on silver nanoparticles synthesized using *Ziziphus Spina–Christi* leaf extract and their antibacterial activity. Phys Conf Ser 2021;1900:012005
32. Mankad M. Patil G, Patel D, Patel P, Patel A. Comparative studies of sunlight mediated green synthesis of silver nanoparaticles from *Azadirachta indica* leaf extract and its antibacterial effect on *Xanthomonas oryzae* pv. oryzae, Arab J Chem 2020;13(1):2865-2872.
33. Khalil MM, Ismail EH, El-Baghdady KZ, Mohamed D. Green synthesis of silver nanoparticles using olive leaf extract and its antibacterial activity. Arub J Chem 2014;7(6):1131-9.

34. Htwe YZN, Chow WS, Suda Y, Mariatti M. Effect of silver nitrate concentration on the production of silver nanoparticles by green method. Mater Today: Pro 2019;17(3):568-73.
35. Rathinavel S, Saravanakumar SS. Synthesis of silver nanoparticles through orange peel powder for antibacterial composite filler applications. J Polym Environ 2022;1-8.
36. Mamdooh NW, Naeem GA. The effect of temperature on green synthesis of silver nanoparticles. AIP Conf Proc 2022;2450.
37. Darroudi M, Ahmad MB, Zamiri R, Zak AK, Abdullah AH, Ibrahim NA. Time-dependent effect in green synthesis of silver nanoparticles. Int J Nanomedicine 2011;677-81.
38. Raja PB, Rahim AA, Qureshi AK, Awang K. Green synthesis of silver nanoparticles using tannins. Mater Sci-Pol 2014 Sep;32:408-13.
39. Cruz ALD, Buendia NJL, Condes RBJ. Antibacterial activity of cassava *Manihot esculenta* leaves extract against *Escherichia coli.* Am J Environ Sci 2022;1(2):23-30.